N^{13} and C^{11} Range and Angular Distributions from N^{14} on B^{10}

K. S. Toth
Oak Ridge National Laboratory, Oak Ridge, Tennessee*
(Received 18 February 1963)

The range and angular distributions of N^{13} and C^{11} particles resulting from the transfer reactions $B^{10}(N^{14},N^{13})B^{11}$ and $B^{10}(N^{14},C^{13})C^{11}$, respectively, are reported. It is found that in the first reaction N^{13} nuclei originating from transfers to B^{11} excited states are observed at angles larger than angles at which N^{13} particles due to ground-state transfers are observed; also, the peaks of the N^{13} angular distributions shift to larger angles when the bombarding energy is lowered. The investigation of the proton-transfer reaction is limited by the low-kinetic energy of the C^{11} particles at large laboratory angles, where most of them are observed for a bombarding energy of 28.0 MeV. When the incident N^{14} energy is lowered, more C^{11} particles are observed at smaller angles. This variation with bombarding energy is as expected for a recoil particle (i.e., the particle into which the target nucleus is transformed) in a transfer reaction. Experimental results obtained for both reactions are compared with the tunneling mechanism proposed by Breit for nucleon transfer.

INTRODUCTION

SINGLE-NUCLEON transfer reactions leading to discrete final states have recently been investigated[1–3] in the irradiation of thin nitrogen and boron targets with 28.0-MeV N^{14} ions. Also, a recent study[4] of the reaction $Mg^{24}(N^{14},N^{13})Mg^{25}$ has been carried out in which N^{13} range and angular distributions were determined. While transfers to discrete Mg^{25} states were not distinguished, some idea was obtained of the Mg^{25} states involved in the reaction. In the present investigation the angular distributions and ranges were determined at various N^{14} incident energies for N^{13} and C^{11} particles resulting from the two reactions: $B^{10}(N^{14},N^{13})B^{11}$ and $B^{10}(N^{14},C^{13})C^{11}$. The purpose was to increase the information available concerning transfer reactions induced by 28.0-MeV N^{14} ions.

EXPERIMENTAL METHOD

Nitrogen-14 ions were accelerated in the Oak Ridge 63-in. cyclotron to an energy[5] of 28.0 MeV. The targets were prepared[6] from boron enriched in B^{10} to 90%. The main impurities in the targets were: carbon, oxygen, silicon, and iron.[3] The two targets used in the investigation were weighed and found to be 65 and 100 $\mu g/cm^2$, or about 0.36 and 0.56 MeV thick, respectively, to the N^{14} beam.

Angular distributions were obtained by stopping the N^{13} and C^{11} particles in circular strips of aluminum foil, each encompassing a known angular increment. These strips were then counted under shielded and calibrated Geiger counters. The amount of N^{13} (10 min) and of C^{11} (20 min) present in each strip was determined from the decay curve. Integral range curves were obtained by varying the quantity of aluminum absorber placed before the circular catchers. A more complete description of the experimental procedure has been published previously.[2]

EXPERIMENTAL RESULTS: $B^{10}(N^{14},N^{13})B^{11}$; $Q=0.91$ MeV

The N^{13} integral range curves obtained at 28.0- and 19.8-MeV N^{14} incident energies are shown in Figs. 1 and 2, respectively. The curves represent N^{13} 10-min activity in each catcher as a function of the quantity of alumi-

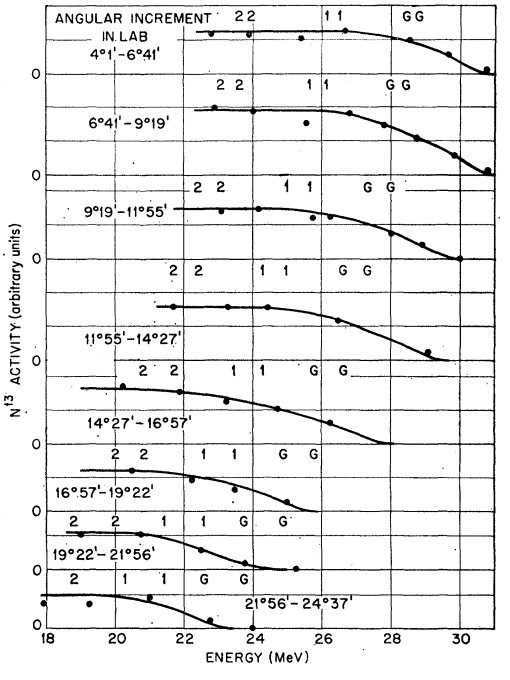

FIG. 1. N^{13} integral range curves obtained at 28.0 MeV. Ordinate scales express N^{13} activity in arbitrary units which also apply to the curves obtained at 19.8 MeV (see Fig. 2). The quantity of absorber has been converted to the corresponding N^{13} energy in MeV. The letter G and the numerals 1, 2, and 3, placed over the curves, indicate N^{13} energies calculated for reactions leaving the B^{11} in various final states; G stands for the ground state, 1 for the first excited state, etc.

* Operated for the USAEC by Union Carbide Corporation.

[1] K. S. Toth, Phys. Rev. **121**, 1190 (1961).
[2] K. S. Toth, Phys. Rev. **123**, 582 (1961).
[3] E. Newman, Phys. Rev. **125**, 600 (1962).
[4] K. S. Toth, Phys. Rev. **126**, 1489 (1962).
[5] M. L. Halbert and A. Zucker, Phys. Rev. **121**, 236 (1961).
[6] G. R. Hoke and E. Newman, ORNL-3021, 1961 (unpublished).

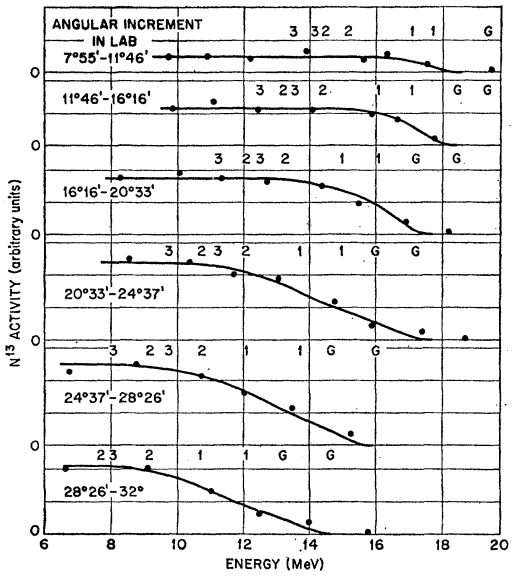

FIG. 2. N^{13} integral range curves obtained at 19.8 MeV. Ordinate scales express N^{13} activity in arbitrary units which also apply to the curves obtained at 28.0 MeV (see Fig. 1). The quantity of absorber has been converted to the corresponding N^{13} energy in MeV. The letter G and the numerals 1, 2, and 3, placed over the curves, indicate N^{13} energies calculated for reactions leaving the B^{11} in various final states; G stands for the ground states, 1 for the first excited state, etc.

num absorber interposed between target and catcher. The amount of absorber has been converted to the energy of an N^{13} particle which would be stopped in that quantity of aluminum. To perform this conversion the experimental range-energy curve of Webb *et al.*[7] for N^{14} particles in aluminum was used; N^{13} and N^{14} ranges at these energies are essentially identical.[8] In Figs. 1 and 2 the letter G and the numbers 1, 2, and 3 placed over the curves indicate the N^{13} energies calculated for transfers leaving B^{11} in various final states; G stands for the B^{11} ground state, 1 for the first excited state, etc. Two sets of N^{13} energies are determined, one for each extreme angle encompassed by the catcher foil.

The range curves level off, indicating that transfers to higher B^{11} states do not occur. Only B^{11} final states are considered because N^{13} excited states are unstable with respect to particle emission; therefore, the detected N^{13} nuclei have been necessarily formed in their ground state. Figure 1 shows that at the forward angles only the ground state of B^{11} contributes to the transfer reaction, while at larger angles the range curves do not level off until the first excited state is included. In fact, transfers to this state only are apparent in the angular range $\sim 17°$ to 24.5° (lab system). The range curves obtained at 19.8 MeV (Fig. 2) show no ground-state contributions, even in the forward angles; only first excited-state transfers are observed at small angles. At larger angles the second and third excited states of B^{11} begin to contribute. While some N^{13} activity is present at energies calculated for ground-state transfers, this activity is probably due to excited-state transfers in which the energy spread is mostly due to the large angular increments.

The factors contributing to the energy uncertainty of the N^{13} particles will now be discussed. The discussion will be limited to the experimental range curves shown in Fig. 1 and taken at the forward angular increments where only the ground state of B^{11} participates in the reaction. In this manner the additional uncertainty due to the presence of N^{13} particles resulting from transfers to several B^{11} states is eliminated. Two independent factors produce a large uncertainty: (1) the N^{14} beam width, and (2) the errors involved in the transformation of the amount of aluminum absorber to the corresponding N^{13} energy. The full width of the N^{14} beam at half-maximum was found to be 1 MeV; the total beam spread was found to be $\sim\pm 1$ MeV. Uncertainties in the range-energy curve,[6] ± 0.1 mg/cm^2, and in the weighing of absorber foils, ± 0.05 mg, can introduce an error of ± 0.9 MeV in the conversion of absorber to N^{13} energy. Smaller errors are introduced by (1) the finite collimator size, which accounts for an uncertainty of $\sim\pm 30$ min in the lab angle and a resultant error of ± 0.15 MeV in the N^{13} energy; (2) multiple scattering of the N^{14} ions in the thin B^{10} target, which was estimated to introduce a negligible error of ± 5 min in the laboratory angle, and, (3) straggling of nitrogen ions in aluminum, which was calculated to be ~ 0.03 mg/cm^2 or ~ 0.2 MeV for nitrogen nuclei in this energy range. An additional error which could be substantial is that introduced by the nonuniformity of the aluminum absorber foils. In Fig. 1 the integral range curves indicate N^{13} activity at some 1.5 MeV beyond the

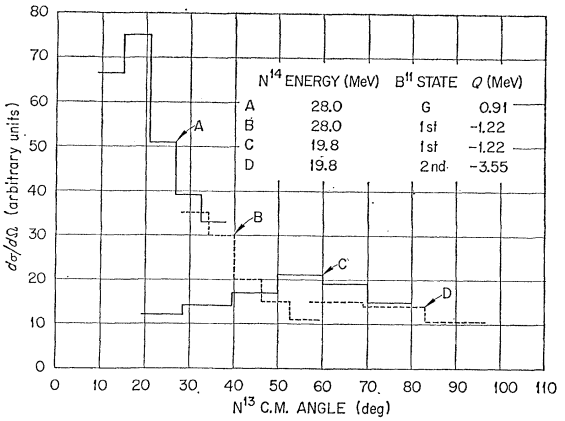

FIG. 3. Angular distributions of N^{13} particles from the reaction $B^{10}(N^{14},N^{13})B^{11}$ at 28.0- and 19.8-MeV bombarding energies. From the range curves in Figs. 1 and 2 it is known that at certain angles more than one B^{11} state is involved in the transfer reaction. For such angles $d\sigma/d\Omega$ was calculated for each B^{11} state by assuming that the transfer proceeded to that state alone.

[7] W. H. Webb, H. L. Reynolds, and A. Zucker, Phys. Rev. **102**, 749 (1956).
[8] L. C. Northcliffe (private communication).

highest calculated N^{13} energy for a given angular increment. This N^{13} spread is within the realm of the errors discussed above.

From the data displayed in the two figures, the differential cross section, $d\sigma/d\Omega$, was calculated as a function of $\theta_{c.m.}$, as shown in Fig. 3. At angles where more than one B^{11} state participated in the transfer reaction, $d\sigma/d\Omega$ was calculated for each state by assuming that the transfer proceeded to that state alone. Two points may be derived from the angular distribution in Fig. 3: (1) N^{13} particles resulting from transfers to excited states are detected at angles larger than those at which ground-state transfer N^{13} nuclei are observed, and (2) the angular distributions shift to larger angles when the bombarding energy is lowered.

The angular distributions in Fig. 3 were integrated and from the target thickness the included cross section was determined to be 3.4 and 3.2 mb for the 28.0- and 19.8-MeV data, respectively. Because the angular ranges studied were too small to include all N^{13} particles, these numbers are less than the measured total cross sections for the reaction, which have been found to be 4.7 mb at the two N^{14} incident energies.[9] During the search for C^{11} activity, larger angles were investigated, N^{13} was also detected, and an estimate was made of the portion of the cross section for the reaction $B^{10}(N^{14},N^{13})B^{11}$ that had been missed previously. The additional N^{13} activity accounted for 0.7 and 1.2 mb at 28.0 and 19.8 MeV, respectively. The total cross sections then become 4.1 and 4.4 mb at the two bombarding energies; this is in satisfactory agreement with the previous measurements.[9]

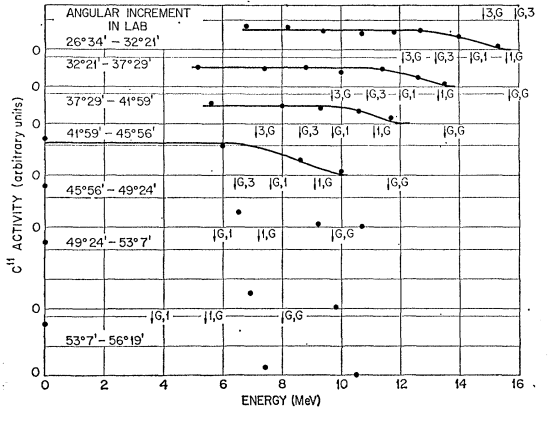

FIG. 4. C^{11} integral range curves obtained at 28.0 MeV. Ordinate scales express C^{11} activity in arbitrary units which also apply to the curves obtained at 19.8 and 14.0 MeV (see Figs. 5 and 6). The quantity of absorber has been converted to the corresponding C^{11} energy in MeV. Arrows placed over the curves indicate C^{11} energies calculated for various combinations of C^{11} and C^{13} final states: G,G signifies C^{11} and C^{13} ground states, 1,G stands for C^{11} first excited state and C^{13} ground state, etc.

[9] M. L. Halbert, T. H. Handley, J. J. Pianjian, W. H. Webb, and A. Zucker, Phys. Rev. **106**, 251 (1957).

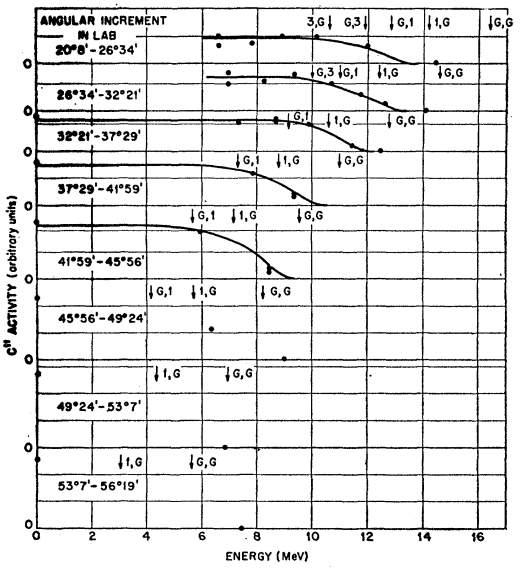

FIG. 5. C^{11} range curves obtained at 19.8 MeV. Ordinate scales express C^{11} activity in arbitrary units which also apply to the curves obtained at 28.0 and 14.0 MeV (see Figs. 4 and 6). The quantity of absorber has been converted to the corresponding C^{11} energy in MeV. Arrows placed over the curves indicate C^{11} energies calculated for various combinations of C^{11} and C^{13} final states: G,G signifies C^{11} and C^{13} ground states, 1,G stands for C^{11} first excited state and C^{13} ground state, etc.

EXPERIMENTAL RESULTS: $B^{10}(N^{14},C^{13})C^{11}$; $Q=1.14$ MeV

We have chosen to refer to C^{11} as the recoil particle despite the fact that it is actually the detected particle. This is done so as to retain the notation used in previous transfer-reaction studies. The target and the nucleus to which it transforms are written outside the parentheses, while the oncoming N^{14} and the nucleus it becomes are written inside, thus: $B^{10}(N^{14},C^{13})C^{11}$. Carbon-11 as the recoil particle in the reaction is expected to act in a manner reverse to that of C^{13} (or N^{13} of the neutron-transfer reaction discussed in the previous section). The recoil particle should be found at large angles when C^{13} is detected at small angles, and when the bombarding energy is lowered the recoil C^{11} should begin to appear at smaller angles. This variation with energy is important if C^{11} is to be detected since its kinetic energy at large angles is barely sufficient for it to leave the B^{10} target.

The C^{11} integral range curves are shown in Figs. 4, 5, and 6. At backward angles the data are quite sketchy due to the low C^{11} velocities and the lack of convenient absorbers. Curves at those angles are not drawn and conclusions are based only on the obvious absence of C^{11} particles resulting from transfers to particular states. The absorber thicknesses were converted to C^{11} energies from the curves of Northcliffe.[8] Zero-absorber points were obtained by counting the absorbers themselves. Another problem arose due to the interference of the 10-min N^{13} activity which predominated over the C^{11}

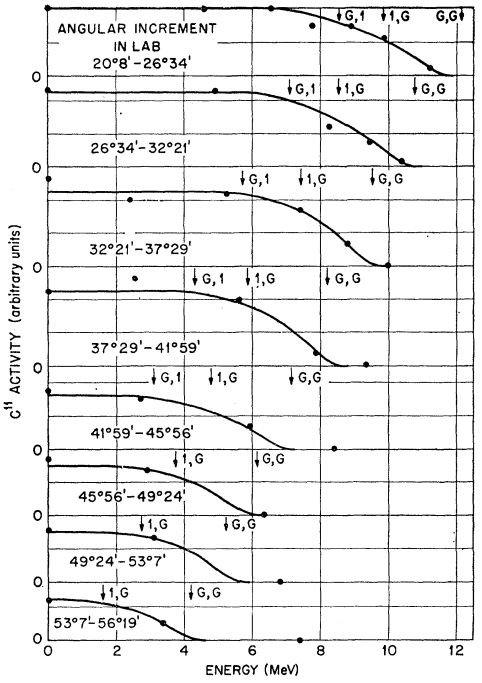

FIG. 6. C^{11} range curves obtained at 14.0 MeV. Ordinate scales express C^{11} activity in arbitrary units which also apply to the curves obtained at 28.0 and 19.8 MeV (see Figs. 4 and 5). The quantity of absorber has been converted to the corresponding C^{11} energy in MeV. Arrows placed over the curves indicate C^{11} energies calculated for various combinations of C^{11} and C^{13} final states: G,G signifies C^{11} and C^{13} ground states, 1,G stands for C^{11} first excited state and C^{13} ground state, etc.

activity at certain angles. When this occurred a large error was introduced in the determination of the amount of C^{11} from the analyses of decay curves. The problem existed for small angles at 28.0 and 19.8 MeV and for larger angles at 14.0 MeV. Large angular increments were necessarily used to give statistically meaningful decay curves. Only the average calculated C^{11} energies are shown for each catcher foil. The arrows in Fig. 4–6 indicating these energies are labeled (G and 1, 2, 3) to indicate the combinations of C^{11} and C^{13} states for which the energies have been calculated. Note that excited states in both residual nuclei, C^{11} and C^{13}, are stable with respect to particle emission. Each arrow is labeled twofold: G,G signifies C^{11} and C^{13} ground states, 1,G signifies C^{11} first excited state and C^{13} ground state, etc.

The 28-MeV data show no G,G transfers; this is in agreement with the 27.5-MeV results of Newman[3] who saw no C^{13} particles resulting from transfers leaving both residual nuclei in their ground states for angles $\gtrsim 40°$ c.m. This angular limit corresponds to $\lesssim 67°$ lab for the recoiling C^{11}. It is to be noticed that: (1) C^{11} nuclei resulting from transfers to high excited states appear at the more forward angles, and (2) when the bombarding energy is lowered, more C^{11} nuclei begin to appear at smaller angles. Both effects are as expected for the recoil particle of a transfer reaction.

The range data were converted to angular distributions, as shown in Fig. 7. The differential cross sections are plotted as a function of the C^{13} center-of-mass angle to facilitate comparison with the results of Newman[3] and with our own experimental data where N^{13} is the detected particle. The range curves clearly show several states in C^{11} and C^{13} participating in the reaction. Because of our inability to resolve the contributions to these states, the angular distributions were determined for the two most probable C^{11} and C^{13} residual state combinations at each bombarding energy. As noted in the previous paragraph, the range data indicate more C^{11} particles at smaller angles when the bombarding energy is lowered. This variation is reflected in the C^{13} angular distributions, i.e., the distributions shift to larger angles at lower incident energies.

DISCUSSION

To compare the angular distributions with the tunneling theory of Breit[10–13] the data shown in Figs. 3 and 7 were replotted as $d\sigma/dR_{\min}$ vs $R_{\min}$, as first sug-

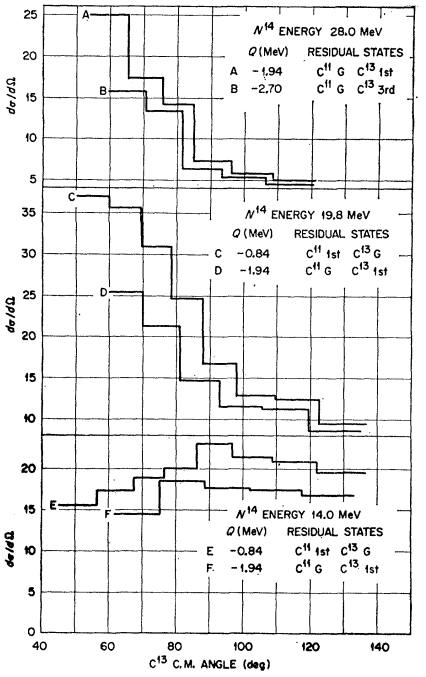

FIG. 7. Angular distributions of C^{13} particles from the reaction $B^{10}(N^{14},C^{13})C^{11}$ at 28.0, 19.8, and 14.0 MeV bombarding energies. At each energy, distributions are drawn for the two most probable C^{11} and C^{13} final-state combinations, as determined from the C^{11} range curves shown in Figs. 4, 5, and 6.

[10] G. Breit and M. E. Ebel, Phys. Rev. **103**, 679 (1956).
[11] G. Breit, in *Handbuch der Physik*, edited by S. Flügge (Springer-Verlag, Berlin, 1959) Vol. XLI, Part 1, pp. 367–407.
[12] G. Breit, in *Proceedings of the Second Conference on Reactions Between Complex Nuclei*, edited by A. Zucker, E. C. Halbert, and F. T. Howard (John Wiley & Sons, Inc., New York, 1960), pp. 1–15.
[13] G. Breit and M. E. Ebel, Phys. Rev. **104**, 1030 (1956).

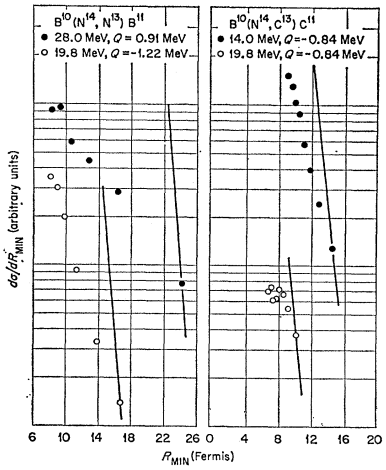

FIG. 8. Angular distribution data of Figs. 3 and 7 plotted as $d\sigma/dR_{\min}$ vs $R_{\min}$. The lines, normalized to the experimental data, are drawn with slopes calculated from the tunneling theory of Breit.

gested by Breit.[12] $R_{\min}$ is the distance of closest approach for a classical trajectory:

$$R_{\min}=(Z_1Z_2e^2/2E_{\text{c.m.}})[1+\csc(\theta/2)]. \quad (1)$$

From the above relation it can be shown that $d\sigma/dR_{\min}$ is proportional to $(d\sigma/d\Omega)[\sin^3(\theta/2)]$. The tunneling theory predicts the small-angle slope of the angular distribution and, therefore, the $d\sigma/dR_{\min}$ slope at large $R_{\min}$. The theory includes the factor $\exp[-\alpha R_{\min}-\bar{\alpha}\bar{R}_{\min}]$, which is plotted vs $R_{\min}$ to obtain the theoretical slope. Here,

$$\alpha=\left(\frac{2M}{\hbar^2}E_s\right)^{1/2}, \quad \text{and} \quad \bar{\alpha}=\left(\frac{2M}{\hbar^2}\bar{E}_s\right)^{1/2}. \quad (2)$$

E_s is the separation energy of the transferred nucleon in the delivering nucleus, $\bar{E}_s=E_s+Q$, and M is the mass of the transferred nucleon. $\bar{R}_{\min}$ is calculated in the same way as $R_{\min}$ but by using $[E_{\text{c.m.}}+Q]$ instead of $E_{\text{c.m.}}$. The theoretical curves are drawn normalized to the data. In Fig. 8 the ordinate scales are in arbitrary units, the purpose being simply to compare the shapes of the angular distributions with those predicted from theory. The comparison was made bearing in mind that the theory, as formulated, is applicable only to the transfer of neutrons, not protons and, only at incident energies below the Coulomb barrier. The experimental slopes, in all instances, are less steep than the theoretical ones. The discrepancy is particularly great for the 28.0-MeV neutron-transfer data. The fit becomes better at 19.8 Mev, as expected, since one is now closer to the energy region (<17.7 MeV) where the tunneling theory is designed to apply. Also, it should be stated that Breit and collaborators[11–13] have proposed and shown that virtual Coulomb excitation, as an additional mechanism, could account for discrepancies between the tunneling theory and experimental results obtained with B^{10} and N^{14} targets.

The peak in a $d\sigma/dR_{\min}$ vs $R_{\min}$ plot is presumably related to the most probable distance for transfer. This distance can be converted to the parameter $r_0(R_{\min}=r_0[A_1^{1/3}+A_2^{1/3}])$, which then may be compared to values of r_0 obtained in other studies. The distributions shown in Fig. 8 are drawn with the assumption of only one Q value/distribution, though it is known that at some angles reactions with more than one Q value occur. If the contributions due to the various Q values could be distinguished and sorted out, the distributions would exhibit maxima. A lower limit of $R_{\min}$ was estimated for the neutron-transfer reaction proceeding to the B^{11} ground state, $R_{\min}>8.8$ F, or $r_0>1.9$ F. The $R_{\min}$ lower limit was arrived at because no N^{13} particles due to ground-state transfers were observed beyond the angle corresponding to that $R_{\min}$. The r_0 limit, >1.9 F, is to be compared with the value of 2.2 F obtained for three other transfer reactions in which both products are left in their ground states.[2,3] The proton-transfer data obtained at 19.8 MeV indicate a maximum at $R_{\min}\approx 7.5$ F or $r_0\approx 1.65$ F. Due to our inability to resolve the different Q-value contributions no attempt was made to determine r_0 values for the other distributions shown in Fig. 8.

Transfers leaving one or both residual nuclei in excited states are observed at angles larger than those at which ground-state transfers are seen; the larger angles correspond to smaller r_0 values. For transfers where the Q value is quite different from zero it is not clear whether a correlation can be made between the angle at which $d\sigma/d\Omega$ peaks and the distance of closest approach. Carbon-13 and N^{13} particles resulting from transfers with Q values quite different from zero would be deflected more than those from ground-state transfers. This does not necessarily mean, however, that the transfer took place when the interacting nuclei were closer together than in the case of a ground-state transfer.

ACKNOWLEDGMENTS

The author wishes to thank M. L. Halbert, E. Newman, and A. Zucker for their comments and helpful discussions. The bombardments were performed by H. L. Dickerson and A. W. Riikola. The apparatus was built by J. G. Harris. Thanks are also due to G. A. Palmer for his assistance in processing data.